New insights on post-myocardial infarction ventricular tachycardia ablation: defining patient-tailored endpoints to improve outcome

De Riva Silva, M.

5

Targeting the hidden substrate unmasked by right ventricular extrastimulation improves ventricular tachycardia ablation outcome after myocardial infarction.

Marta de Riva, MD, PhD, Yoshihisa Naruse, MD, PhD, Micaela Ebert, MD, Alexander F.A. Androulakis, MD, Qian Tao, PhD, Masaya Watanabe, MD, PhD, Adrianus P. Wijnmaalen AP, MD, PhD, Jeroen Venlet, MD, Charlotte Brouwer, MD, Serge A. Trines, MD, PhD, Martin J. Schalij, MD, PhD, Katja Zeppenfeld, MD, PhD

JACC: Clinical Electrophysiology 2018;4:316-327

ABSTRACT

Background

In patients with small or non-transmural scars after myocardial infarction (MI), part of the ventricular tachycardia (VT) substrate might be functional and, in addition, masked by high voltage far-field signals arising from adjacent normal myocardium.

Objectives

To determine whether ablation of hidden substrate unmasked by right ventricular extrastimulation (RVE) improves ablation outcome

Methods and Results

In sixty consecutive patients, systematic analysis of electrograms recorded from the presumed infarct area was performed during sinus rhythm, RV pacing at 500ms and during a short coupled RV extrastimulus. Sites showing low voltage, near-field potentials *wit*h evoked conduction delay in response to RVE were targeted. In 37 patients (62%), ablation target sites located in areas with normal voltage during sinus rhythm were unmasked by RVE (hidden substrate group). These patients had better LV function (36±11% vs. 26±12%; P=0.003), smaller electroanatomical scars (<1.5mV) and smaller dense scars (<0.5mV) (median 59 and 14 vs. 82 and 44 cm^2; P=0.044 and P=0.003) than those in whom no hidden substrate was identified (overt substrate group). During a median follow-up of 16 months, 13 patients (22%) had VT recurrence. Patients with hidden substrate had a lower incidence of VT recurrence (12 month VT-free survival 89% vs 50% in patients with overt substrate; P=0.005). Compared to a historical cohort of 90 post-MI patients matched for LV function and electroanatomical scar area, in whom no RVE was performed, patients in the hidden substrate group had a higher 1-year VT free survival (89% vs 73%; P= 0.039).

Conclusion

Hidden substrate ablation unmasked by RVE improves ablation outcome in post-MI patients with small or non-transmural scars.

INTRODUCTION

Substrate-based ablation for post-myocardial infarction (MI) ventricular tachycardia (VT) relies on: 1) delineation of low bipolar voltage (BV) areas (<1.5mV) by electroanatomical (EA) mapping and 2) identification of electrograms (EGMs) consistent with slow conduction or conduction block within low-voltage areas during sinus rhythm (SR).(1,2) Mapping accuracy to detect scar might, however, be limited by the current use of ablation catheters with large electrodes and wide inter-electrode spacing leading to far field contamination of local EGMs.(3) This phenomenon might be particularly relevant in patients with smaller and subendocardial scars, in whom parts of the arrhythmogenic substrate may be obscured by high-voltage far-field signals arising from adjacent normal myocardium. Of note, this scar pattern is often encountered in contemporary patients undergoing early reperfusion therapy, associated with fast and poorly tolerated VT.(4,5) The inability of BV mapping during SR to delineate non-transmural scars has been demonstrated by head-to-head comparison of voltage maps with contrast-enhanced magnetic resonance imaging (CE-MRI).(5) Changing the activation wavefront by continuous ventricular pacing may identify low-voltage areas that are not evident during SR.(6) However, using EGM amplitude as only guide may lead to unnecessary ablation with potential damage of viable myocardium contributing to cardiac function. Critical sites for VT should exhibit additional electrophysiological characteristics, most importantly functional conduction delay or conduction block.

We hypothesized that: 1) systematic evaluation of EGMs located in the infarct area during right ventricular extrastimulation (RVE) can identify scar areas with functional conduction delay or block as substrate for VT that are not evident during SR and 2) ablation targeting this hidden, functional substrate may improve ablation outcome in post-MI patients.

METHODS

Between October 2013 and February 2016, consecutive post-MI patients referred for VT ablation to the Leiden University Medical Center were prospectively included. All patients were treated according to the institutional clinical protocol and provided pre-procedural informed consent.

Preprocedural evaluation

Patients underwent a comprehensive clinical evaluation including review of all medical records. Data on past ischemic events, acute reperfusion therapy, prior revascularize-

tion, spontaneous ventricular arrhythmias, implantable cardioverter-defibrillator (ICD) interrogation reports and failed anti-arrhythmic drugs (AAD) were collected. All patients underwent coronary angiography or non-invasive stress testing to detect ischemia. Coronary angiograms were reviewed to determine the area supplied by the infarct-related artery. Wall motion abnormalities and left ventricular (LV) function were derived from echocardiograms. If possible, CE-MRI was performed for scar delineation (Supplementary Methods 1).(7) Patients scheduled for epicardial ablation underwent ECG-gated cardiac computed tomographic imaging for procedural integration.(8) Before ablation, all AAD with the exception of amiodarone were discontinued**.**

Ablation procedure

Prior to ablation, programmed electrical stimulation (PES) was performed (4 drive cycle lengths [S1, CL: 600, 500, 400 and 350ms], 1-4 ventricular extrastimuli [S2, ≥200ms] from 2 RV sites and ≥1 LV site). Positive endpoint of stimulation was induction of sustained VT lasting > 30s or requiring termination because of hemodynamic compromise. Fast VT was defined as a VT with CL ≤ventricular refractory period (VRP) + 30ms. (9)

Electroanatomical mapping

All patients underwent LV endocardial mapping. Additional RV and/or epicardial mapping was performed if appropriate. BV maps were created with a 3.5mm irrigated-tip catheter (NaviStar ThermoCool; Biosense Webster, Inc, Diamond Bar, CA) and the CARTO 3 system. Standard cut-off values of 1.5mV for scar, 0.5mV for dense scar and 0.5-1.5mV for border-zone were applied. A patchy scar pattern was defined as two low-voltage areas separated by areas of preserved voltage. (4) CE-MRI derived scars were integrated with EA maps as previously described. (7)

Electrogram analysis

Bipolar EGMs were filtered at 30-500Hz and displayed at a gain of 0.072 mV/cm and a sweep speed of 200mm/s on the Prucka EP system. With the mapping catheter in a stable position, EGMs were systematically analysed during SR, RV pacing at a fixed rate of 500ms and during the application of a single RV extrastimulus (RVe) with a coupling interval of 50ms above the VRP. Care was taken to cover the presumed infarct area as derived from imaging data (echocardiogram and CE-MRI) and review of coronary angiogram, regardless of local EGM amplitude or morphology during SR.

During SR, the peak-to-peak EGM amplitude was automatically determined by the CARTO 3 system. If during RV pacing, the local EGM showed two distinct components, a low-frequency potential consistent with far-field EGM and a single or multicomponent high-frequency potential consistent with near-field EGM, the amplitude of the near-field

was manually measured on the EP system using electronic callipers. Subsequently, EGM duration, measured as the interval between the earliest and the last sharp deflections,(2) during the pacing train and the RVE was compared. Sites exhibiting low-amplitude (<1.5mV) near-field potentials with conduction delay >10ms or block in response to RVE were categorized as Evoked Delayed Potentials (EDP) and annotated on the map (**Figure 1**)**.**

Ablation

Substrate modification aiming EDP elimination was performed. Late potentials (LP, onset after QRS, separated by an isoelectric segment from the far-field signal >20ms) during SR or RV pacing without additional conduction delay during RVE were not targeted. Radiofrequency (RF) energy was delivered (45-50W, temperature limit 43ºC, flow rate 20-30 ml/min) until stimulation with high output pacing (10 mA, 2ms) failed to capture. After the last RF application, a re-map including RVE was performed and the entire induction protocol was repeated. Fast VTs with a CL close to VRP were considered clinically not relevant and not targeted. If any other sustained monomorphic VT remained inducible, additional mapping and ablation was performed until no further substrate could be identified.

Post-procedural management and follow-up

Patients underwent routine echocardiogram to exclude pericardial effusion and assess post-ablation LV function. ICD implantation was offered to those without a device before ablation. Pre-procedural AADs were continued until the first follow-up visit. Patients were followed at 3 months post-ablation and every 6 months thereafter. VT recurrence was defined as occurrence of any VT requiring ICD therapy, recorded within the ICD monitor zone lasting >30s or documented on 12-lead ECG.

Long-term outcome comparison with historical group

For long-term outcome comparison, a historical cohort of consecutive ischemic patients who underwent VT ablation in the same institution between 2009 and 2012 was used. In this period, RVE for substrate identification was not performed and ablation target sites were selected based on a combination of activation and entrainment mapping, pace-mapping and substrate mapping (identification of fragmented EGMs and LPs during SR). All procedures in the historical and present study group were performed by the same operator, using irrigated-tip ablation catheters and the CARTO system.

Figure 1.
EGM response to RV extra-stimulation

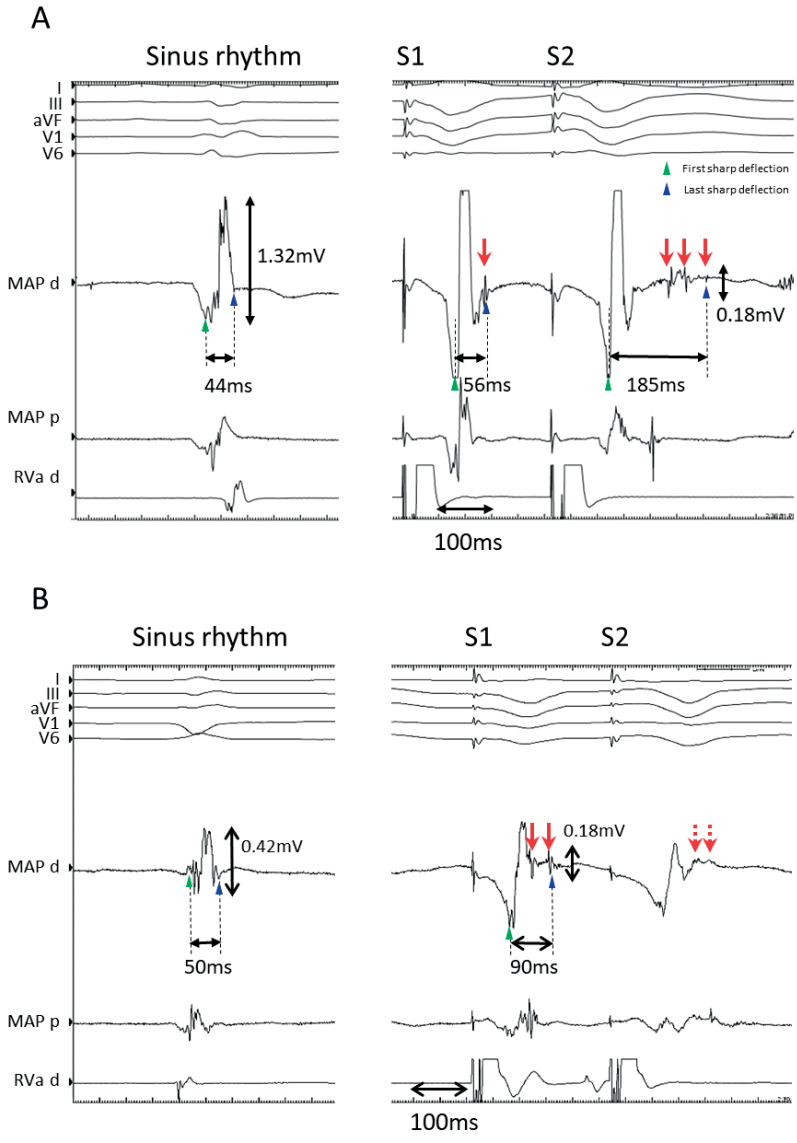

(A) *Evoked delayed potential* (EDP). EGM with borderline amplitude during SR (left). During RV pacing (S1), a low-amplitude high-frequency potential (red arrow) separates from the far-field high-voltage signal (centre). This second component further delays and splits into multiple components during an extrastimulus (S2) (right). (B) EDP. Low-voltage, fragmented EGM during SR (left). Two high-frequency delayed potentials (red arrows) are observed during S1 (centre) which disappeared during S2 (right, dashed red lines). (C) Negative response to RVE. Low-voltage abnormal signal during SR (left). During S1, a high-frequency potential (red arrow) occurred after the far-field signal (centre), which showed no additional conduction delay after S2 (right). (D) EDP. Normal EGM (amplitude and morphology) during SR (left). Low-voltage near-field potential separated from the far-field signal (S1), delaying and splitting in multiple components (S2) (right). (E) Negative response to RVE. Fragmented low-voltage EGM during SR (left). Local conduction delay during S1 (centre) but without further prolongation after S2. All EGM durations measured from first to last sharp deflection irrespective of number of components.

Figure 1.
EGM response to RV extra-stimulation

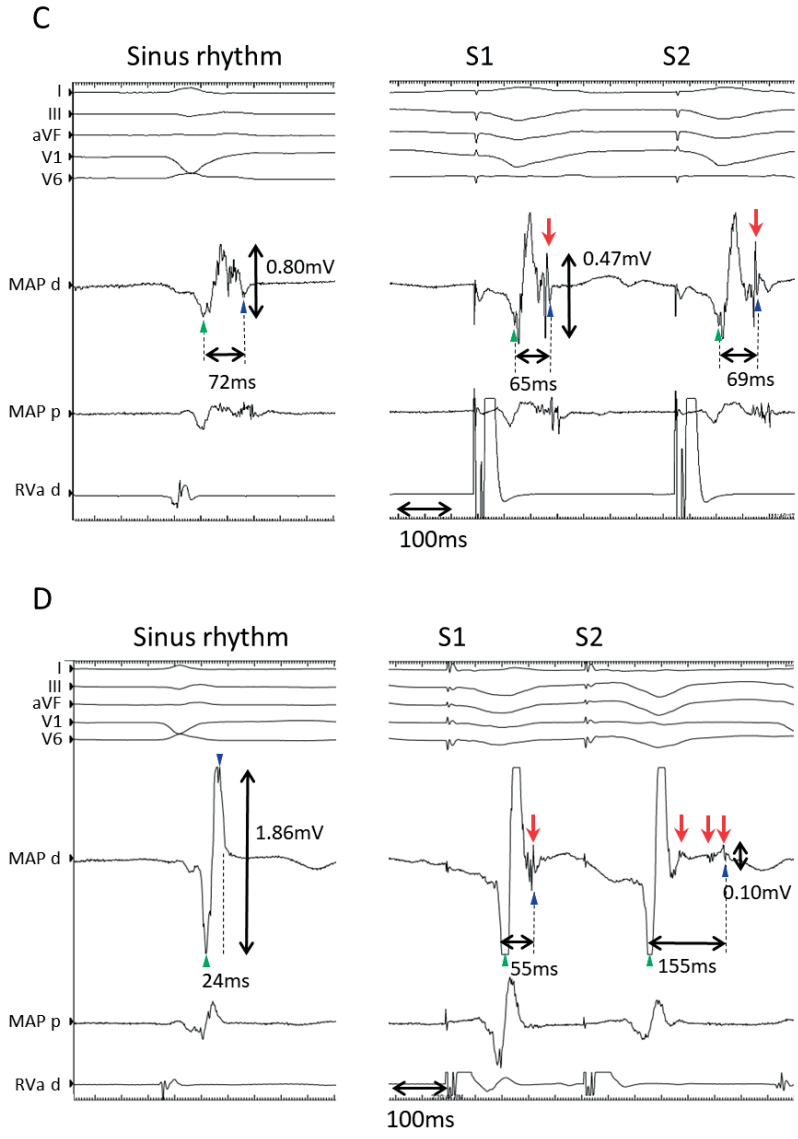

(A) *Evoked delayed potential* (EDP). EGM with borderline amplitude during SR (left). During RV pacing (S1), a low-amplitude high-frequency potential (red arrow) separates from the far-field high-voltage signal (centre). This second component further delays and splits into multiple components during an extrastimulus (S2) (right). (B) EDP. Low-voltage, fragmented EGM during SR (left). Two high-frequency delayed potentials (red arrows) are observed during S1 (centre) which disappeared during S2 (right, dashed red lines). (C) Negative response to RVE. Low-voltage abnormal signal during SR (left). During S1, a high-frequency potential (red arrow) occurred after the far-field signal (centre), which showed no additional conduction delay after S2 (right). (D) EDP. Normal EGM (amplitude and morphology) during SR (left). Low-voltage near-field potential separated from the far-field signal (S1), delaying and splitting in multiple components (S2) (right). (E) Negative response to RVE. Fragmented low-voltage EGM during SR (left). Local conduction delay during S1 (centre) but without further prolongation after S2. All EGM durations measured from first to last sharp deflection irrespective of number of components.

Figure 1.
EGM response to RV extra-stimulation

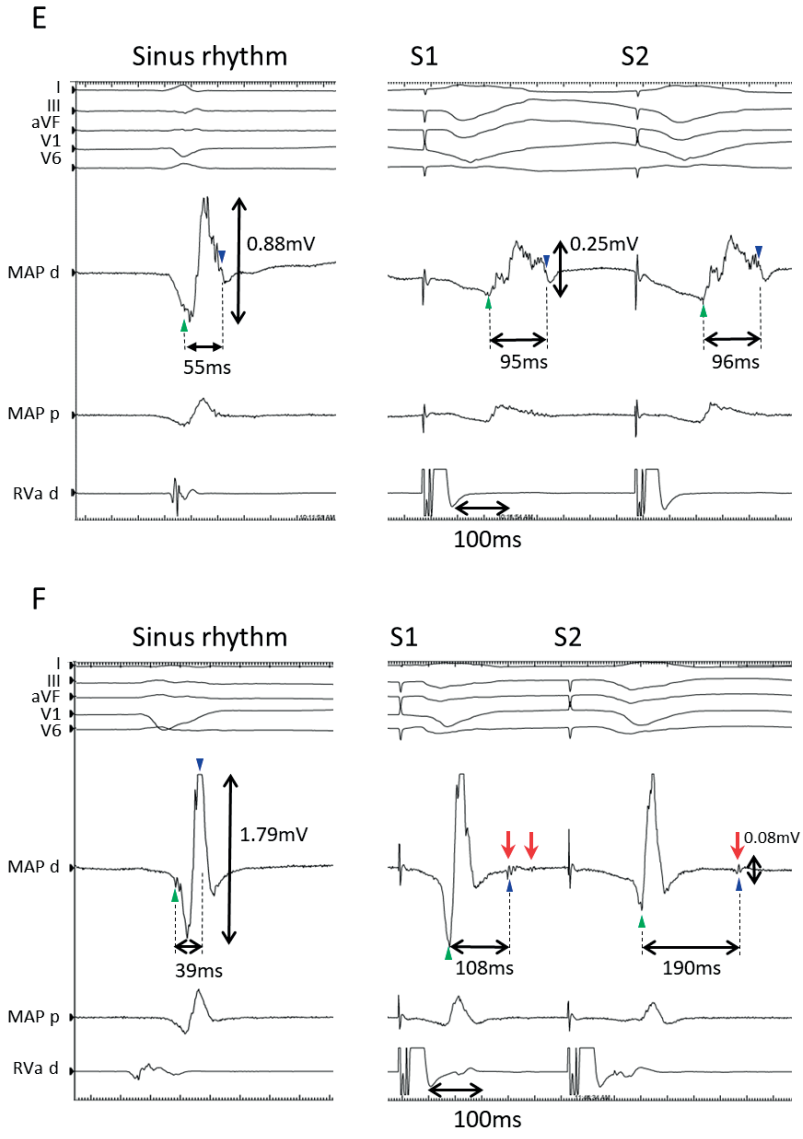

(A) *Evoked delayed potential* (EDP). EGM with borderline amplitude during SR (left). During RV pacing (S1), a low-amplitude high-frequency potential (red arrow) separates from the far-field high-voltage signal (centre). This second component further delays and splits into multiple components during an extrastimulus (S2) (right). (B) EDP. Low-voltage, fragmented EGM during SR (left). Two high-frequency delayed potentials (red arrows) are observed during S1 (centre) which disappeared during S2 (right, dashed red lines). (C) Negative response to RVE. Low-voltage abnormal signal during SR (left). During S1, a high-frequency potential (red arrow) occurred after the far-field signal (centre), which showed no additional conduction delay after S2 (right). (D) EDP. Normal EGM (amplitude and morphology) during SR (left). Low-voltage near-field potential separated from the far-field signal (S1), delaying and splitting in multiple components (S2) (right). (E) Negative response to RVE. Fragmented low-voltage EGM during SR (left). Local conduction delay during S1 (centre) but without further prolongation after S2. All EGM durations measured from first to last sharp deflection irrespective of number of components.

Statistical analysis

Continuous variables are reported as mean±SD or medians with interquartile range (IQR) and compared with the Student's t or the Mann-Whitney U test when appropriate. Categorical variables are expressed as numbers and percentages (%) and compared with the Chi-squared or the Fisher exact test. Freedom from VT recurrence was estimated by Kaplan-Meier method and compared with log-rank test between groups. Cox proportional regression analysis was performed to detect any significant predictor of VT recurrence (reported as the hazard ratio [HR] with a 95% confidence interval [CI]). All tests were 2-sided and a P value <0.05 was considered statistically significant. Statistical analyses were performed with SPSS version 20.0 (SPSS Inc, Chicago, IL).

RESULTS

Patients

During the study period, 62 post-MI patients underwent VT ablation. Two patients with poor hemodynamics in whom the complete pacing protocol could not be performed were excluded. The remaining 60 patients (49 men, 67 ± 8 years, LV ejection fraction (EF) 33 ± 12%) comprised the study population. Baseline characteristics are displayed in **Table 1**. In **Supplementary Table 1**, baseline characteristics of the historical cohort are shown.

PES, electroanatomical mapping and electrogram analysis

Fifty-five patients (92%) were inducible for a median of 3 VTs (IQR 1-4). LV endocardial mapping was performed in all and epicardial and endocardial RV mapping in 6 (12%) and 13 (22%) patients, respectively. Procedural characteristics of the study patients and historical group are shown in **Table 2 and Supplementary Table 2,** respectively.

A total of 2858 bipolar EGMs (median 45 per patient, IQR 27-62) in the presumed infarct area were analysed during SR, RV pacing and RVE. Of these, 1367 (48%) were located in the EA dense scar and 867 (30%) in the border-zone. The remaining 624 EGMs (22%) were located in normal BV areas. During RVE, 930 EGMs (33%) were classified as EDPs (810 (87%) showed EGM prolongation >10ms (median 31ms, IQR 20-46) and 120 (13%) block). Of importance, 184 of 930 EDPs (20%) were located in sites with normal voltage during SR. Details of EGM analyses are displayed in **Table 3**.

Seven patients (12%) underwent integration of CE-MRI derived scars with EA maps. In these patients, a total of 391 EGMs were analysed with RVE and 91 (23%) were categorized as EDPs. Of importance, 34/91 EDPs (37%) were located in areas with normal

BV. However, according to the CE-MRI, 31/34 (91%) were located within the scar and of interest, 22 of 31 (71%) in an area of non-transmural scar.

Table 1. Baseline characteristics of the patients according to left ventricular ejection fraction

	All (n=60)	Hidden Substrate (n=37)	Overt Substrate (n=23)	*P-value*
Age, years	68 ± 8	69 ± 8	66 ± 7	0.237
Male	49 (82%)	31 (84%)	18 (78%)	0.734
Hypertension	19 (32%)	12 (32%)	7 (30%)	1.000
Diabetes Mellitus	10 (17%)	7 (19%)	3 (13%)	0.727
Prior stroke/TIA	5 (8%)	3 (8%)	2 (9%)	1.000
Atrial fibrillation	15 (25%)	11 (30%)	4 (17%)	0.366
Heart failure	24 (40%)	10 (27%)	14 (61%)	0.014
Renal failure	18 (30%)	9 (24%)	9 (39%)	0.177
Inferior MI	36 (60%)	25 (68%)	11 (48%)	0.419
Time since MI, year	19 ± 8	21 ± 9	17 ± 7	0.096
MI acute reperfusion	12 (20%)	7 (19%)	5 (22%)	1.000
Prior CABG	18 (30%)	15 (41%)	3 (13%)	0.041
Prior PCI	24 (40%)	13 (35%)	11 (48%)	0.419
LV ejection fraction, %	33 ± 12	36 ± 11	26 ± 12	0.003
ICD before ablation	50 (83%)	28 (76%)	22 (96%)	0.073
Prior VT ablation	14 (23%)	9 (24%)	5 (22%)	1.000
Clinical VT CL, ms	417 ± 102	404 ± 96	437 ± 109	0.224
Medication at admission				
Statins	53 (88%)	31 (84%)	22 (96%)	0.233
Antialdosteronic	17 (28%)	5 (14%)	12 (52%)	0.003
ACE-I/ARB	46 (77%)	26 (70%)	20 (87%)	0.211
Betablockers	48 (80%)	30 (81%)	18 (78%)	1.000
Amiodarone	22 (37%)	13 (35%)	9 (39%)	0.788
VT clinical presentation				
Electrical storm	7 (12%)	4 (11%)	3 (13%)	1.000
Incessant VT	5 (8%)	2 (5%)	3 (13%)	0.362
ICD therapies	15 (25%)	10 (27%)	5 (22%)	0.764
Below ICD detection	24 (40%)	13 (35%)	11 (48%)	0.419
First episode without ICD	9 (15%)	8 (22%)	1 (4%)	0.134

Values are reported as mean ± standard deviation or n (%). TIA indicates transitory ischemic attack; MI, myocardial infarction; CABG, coronary artery bypass grafting; PCI: percutaneous coronary intervention; LV, left ventricle; ICD, implantable cardiac defibrillator; VT, ventricular tachycardia; CL, cycle length; ACE-I, angiotensin-converting-enzyme inhibitor and ARB, angiotensin receptor blocker.

Table 2. Procedural characteristics

	All (n=60)	Hidden substrate (n=37)	Overt substrate (n=23)	*P-value*
Inducible before RFCA	55 (92%)	36 (97%)	19 (83%)	0.066
Number of induced VTs	3 (1–4)	2 (1–4)	3 (1–4)	0.963
Induced VT max CL, ms	420 ± 103	411 ± 112	438 ± 85	0.354
Induced VT min CL, ms	304 ± 78	293 ± 58	325 ± 105	0.230
LV bipolar scar area, cm^2	64 (41–87)	59 (34–79)	82 (47–106)	0.044
LV dense scar area, cm^2	25 (6–44)	14 (5–32)	44 (24–62)	0.003
LV border zone area, cm^2	34 (23–47)	33 (21–51)	37 (25–47)	0.662
Dense scar area/total LV area, %	10 (3-17)	7 (3-7)	15 (9-15)	0.003
Epicardial mapping	6 (10%)	2 (5%)	4 (17%)	0.027
Procedural duration, min	173 (150–205)	175 (151–205)	167 (150–230)	0.982
Fluoroscopic time, min	39 (33–47)	38 (35–47)	39 (28–48)	0.814
Radiofrequency time, min	15 (10-21)	15 (11-21)	13 (9-21)	0.626
ICD after RFCA	53 (88%)	31 (84%)	22 (96%)	0.233
AADs at discharge				
Amiodarone	23 (38%)	14 (38%)	9 (39%)	1.000
Sotalol	12 (20%)	7 (19%)	5 (22%)	1.000
Class I	1 (2%)	1 (3%)	0 (0%)	1.000

Values are reported as mean ± standard deviation, median and IQR or n (%). RFCA indicates radiofrequency catheter ablation and AAD, antiarrhythmic drugs. Other abbreviations as in Table 1.

Table 3. Electrogram characteristics

	All (n=2858)	Evoked Delayed Potentials (n=930)	Other EGM (n=1928)	*P-value*
EGM location				0.094
Dense scar (<0.5mV)	1367 (48%)	469 (50%)	898 (47%)	
Border zone (0.5–1.49mV)	867 (30%)	277 (30%)	590 (31%)	
Normal voltage area (≥1.5mV)	624 (22%)	184 (20%)	440 (22%)	
EGM characteristics during SR				
Amplitude, mV	0.52 (0.03–25.61)	0.49 (0.04–6.69)	0.54 (0.03–25.61)	0.026
Duration, ms	69 (15–422)	75 (21–288)	65 (15–422)	<0.001
EGM characteristics during RV pacing				
Near-field amplitude (if present), mV	0.09 (0.03–0.93)	0.09 (0.03–0.93)	0.10 (0.04–0.39)	0.486
Duration, ms during S1	70 (19–450)	86 (29–450)	64 (19–308)	<0.001
Duration, ms during S2	79 (11–589)	112 (27–589)	69 (11–296)	<0.001
EGM prolongation from S1 to S2, ms	7 (0–364)	31 (10–364)	4 (0–85)*	<0.001

Values are reported as median and range or n (%). EGM indicates electrogram and RV, right ventricle. EGMs with near-field low voltage signals *and* conduction delay >10ms or conduction block in response to RV extrastimulation were categorized as evoked delayed potentials. *EGM with conduction delay or block by RVE with BV>1.5mV were not considered EDP.

Group definition

Thirty-seven patients (62%) in whom EDPs were identified in areas with normal BV during SR constituted the "*hidden substrate group*". The remaining 23 patients (38%), in whom either no EDP was identified (4/23 [17%]) or only within the EA scar area (19/23 [83%]), conformed the "*overt substrate group*" (**Figure 2**). Patients in the overt substrate group had lower LVEF (26±12% vs. 36±11%; P=0.003), larger scars and dense scars (median 82 [IQR 47-106] and 44 [IQR 24-62]cm^2 vs. 59 [34-79] and 14 [5-32]cm^2; P=0.044 and P=0.003 respectively) and more frequently heart failure (14 (61%) vs 10 (27%); P=0.014). Of note, patients in the hidden substrate group had more often undergone CABG (15 (41%) vs. 3 (13%); P=0.041).

Ablation

The median time of RF was 15 minutes (IQR 10-21). After EDP elimination, 40 patients (67%) did not require any additional ablation. In 14 patients (23%), remaining induced VTs were successfully abolished based on activation, entrainment and/or pace-mapping. Six patients (10%) remained inducible for any targeted VT at the end of the procedure.

Complications

One patient with prior CABG underwent surgical adhesiolysis for epicardial access, which was complicated by a bypass occlusion. The patient died 24h despite surgical revascularization due to a vasoplegic syndrome. Pericardial bleeding requiring percutaneous drainage occurred in 2 patients

Post-procedural management

No patient had deterioration of LV function on post-procedural echocardiogram. Fifty-three patients (88%) were discharged with an ICD. Seven patients (12%) refused ICD implantation (all non-inducible after ablation and LVEF≥ 35%). Thirty-three patients were discharged on AADs (21 patients (57%) in the hidden substrate group vs 12 (52%) in the overt substrate group; P=0.793). In total, 22 patients (38%) were discharged on amiodarone, 12 (20%) on sotalol and 1 (2%) on the combination of amiodarone with mexiletine.

Follow-up

During a median follow-up of 16 months (IQR 8-23), 13 patients (22%) experienced VT recurrence (median time to recurrence 150 days). Patients in the hidden substrate group had a higher 12-month VT free survival (89% [95% CI 78-100] vs 50% [95% CI 24-76] in the overt substrate group; P=0.005) (**Figure 3**). Five patients died after a median of 205 days (3/5 of cardiac causes) and 2 patients received a Left Ventricular Assist Device 12 days and 17 months after ablation. At last follow-up, 35 patients (58%) were on AADs (18

patients (49%) in the hidden substrate group vs 17 (74%) in the overt substrate group; P=0.065).

Figure 2.
Examples of patients of the Overt and Hidden Substrate Groups

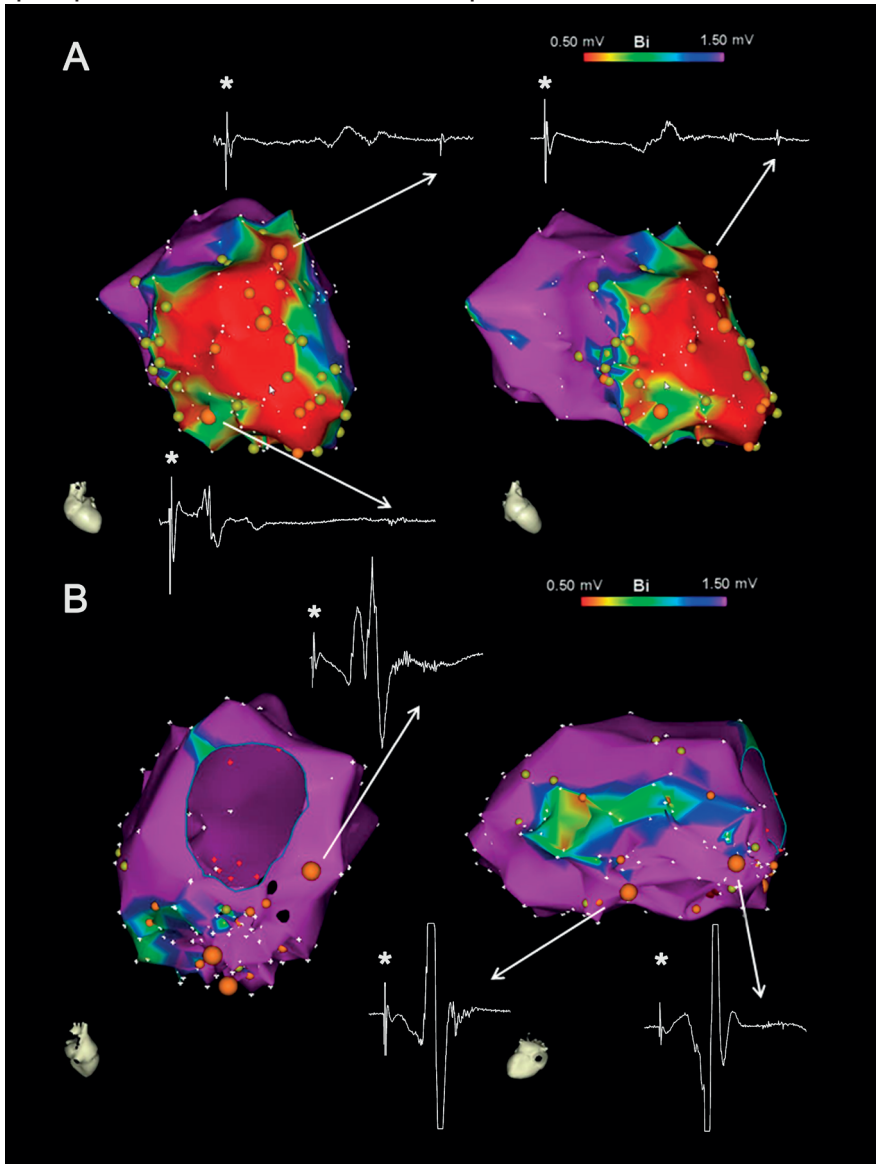

BV maps and local EGMs during RVE (S2) from patients of the overt substrate group (A) and the hidden substrate group (B). BV is color-coded according to bar. Sites with *"evoked delayed potentials" (EDP)* are marked by orange tags. Other pacing sites are marked by yellow tags. Panel A: BV maps in anteroposterior (left) and right anterior oblique (right) views. All EDPs are confined to the low-voltage area. Panel B: BV maps in posterior and inferolateral views. EDPs are also located in areas with normal voltage and unmasked by RVE.

Univariate Cox regression analysis showed that the absence of a hidden substrate (HR 4.63; CI 95% 1.41-15.15: P=0.011), a higher number of induced VTs (HR 1.24 per additional VT; 95% CI 1.01-1.52: P=0.039) and a larger bipolar scar area (HR 1.02 per cm^2; 95% CI 1.0-1.03: P=0.007) were associated with higher incidence of VT recurrence (**Supplementary Table 3**).

Figure 3.

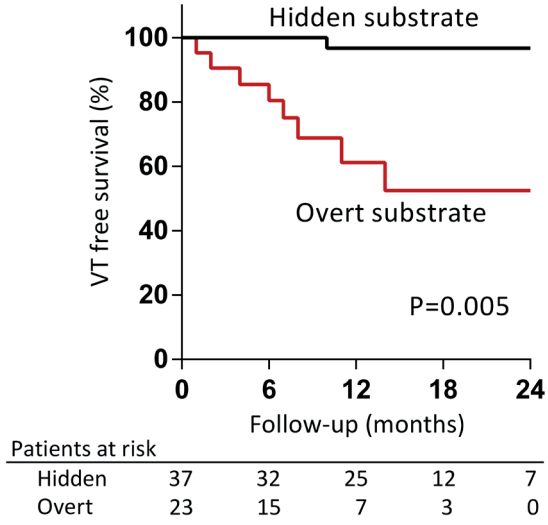

Ventricular tachycardia-free survival in hidden vs. overt substrate groups

Long-term outcome comparison with historical group

Patients from the hidden and overt substrate groups differed in baseline characteristics known to impact the incidence of VT recurrence (LVEF, scar area).(10,11) Therefore, long-term ablation outcome for each group was compared with a LV function and bipolar scar area matched cohort of patients from the historical group who underwent ablation without RVE for substrate identification.

Patients in the overt substrate group had a similar incidence of VT recurrence than patients in the matched historical cohort (12-month VT free survival 66% [95% CI 46-86] vs. 65% [95% CI 45-85]; P=0.608). On the contrary, patients in the hidden substrate group had a better VT-free survival than patients in the matched historical cohort (12-month VT free survival 89% [95% CI 79-99] vs. 73% [95% CI 59-87]; P=0.039), suggesting that substrate identification and ablation based on RVE might be particularly beneficial in post-MI patients with moderately depressed LV function and small and non-transmural scars (**Figure 4**).

Figure 4.

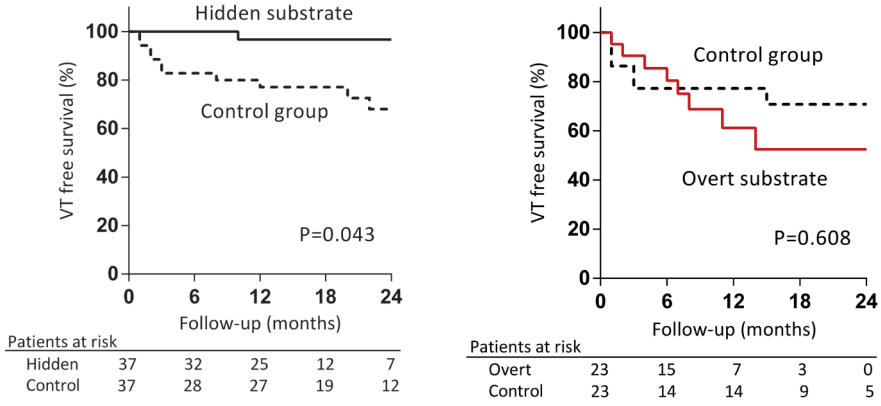

Ventricular tachycardia-free survival in hidden substrate (A) and overt substrate groups (B) vs. LV ejection fraction and bipolar scar area matched historical controls

DISCUSSION

In the present study, we demonstrate that in patients undergoing ablation for post-MI VT, systematic evaluation of EGMs recorded from the presumed infarct area during RVE can unmask areas of scar with functional conduction delay or block. These areas with *evoked delayed potentials* as potential substrate for VT cannot be detected if mapping is performed during SR or continuous RV pacing only. Patients in whom EDP were recorded within normal EA voltage areas had a relatively preserved LV function and small and patchy scars. These hidden substrates were particularly located in areas of non-transmural scar with viable subepicardial myocardium on CE-MRI. The latter can result in “pseudo” normal BV during SR and is important to consider in contemporary patients with acute reperfusion therapy and after prior CABG. Of importance, compared to a LV function and scar area matched historical cohort of post-MI patients in whom substrate identification based on RVE was not performed, patients undergoing ablation of unmasked *hidden substrate* had better VT-free survival after ablation.

Substrate-based ablation for post-MI VT

Substrate-based ablation approaches have been developed for targeting unstable or non-inducible VTs, circumstances that affect 70% and 10% of patients currently referred for ablation of post-MI VT.(10,12) Although substrate-based ablation is superior to ablation limited to clinical or hemodynamically stable VTs, (13) the reported VT recurrence rates after substrate modification remain high (32%-47%). (12,14,15) It has been suggested that the scar size impacts the long-term outcome after ablation. In a prior cohort

of post-MI patients who underwent substrate modification targeting LPs during continuous RV pacing, the presence of a dense scar area >25cm^2 was independently associated with a higher incidence of VT recurrence. Of interest, although patients with small scars (<25cm^2) and slow VTs (CL >350ms) had an excellent prognosis, patients with small scars *and* fast VTs (CL<350ms) had higher recurrence rates, comparable to those with large scars *and* slow VTs (CL >350ms). (12) These findings suggest that, in patients with small scars and a substrate for faster VT, substrate identification during SR or RV pacing might not be sufficient.

Substrate mapping: Delineation of scar area

The cornerstone of substrate-based VT ablation is the delineation of the EA scar using standard BV cut-off values of 1.5mV and 0.5mV for scar and dense scar. (1) Mapping accuracy to detect scar might, however, be hampered by far-field contamination of local low-voltage signals. This might be particularly relevant in the presence of non-transmural scars, typically encountered in patients undergoing acute reperfusion of the infarct related artery (4) or with well-developed collaterals. In these patients, subepicardial viable myocardium overlying the subendocardial scar may generate high voltage far-field signals leading to underestimation of the scar area.(16) Accordingly, a mismatch between non-transmural scar size delineated by voltage mapping and CE-MRI has been demonstrated. (17) In addition, VT termination by ablation beyond the EA scar area has been reported, further emphazising the limitation of BV mapping during SR to identify the entire arrhythmogenic scar. (6) In our study, patients in whom additional areas of scar with local conduction delay were unmasked by RVE had smaller EA scars with either no dense scar (n=2) or only small dense scar areas (involving a median of 7% of the total LV area), suggesting the presence of a non-transmural scar. In fact, in those patients who underwent CE-MRI scar integration with EA maps, 71% of sites showing hidden substrate for VT were located in areas of non-transmural scar. This finding could not be explained by a higher acute revascularization rate in our cohort, which was low in both groups. However, significantly more patients in the hidden substrate group had undergone CABG which may have contributed to improved epicardial collateral coronary flow and the non-transmurality of the scar. The use of narrow-spaced, multipolar catheters and voltage mapping performed during pacing from multiple sites may help to identify additional low-voltage areas not detected during SR. (3,6) However, whether small, narrow-spaced electrodes reduce far-field contamination from the subepicardium for small and patchy scars is unknown. Similarly, whether the change of activation sequence at a fixed CL is sufficient to change the temporal relation between epicardial and subendocardial activation at the recording site in small scars with little activation delay at lower pacing rates, needs further evaluation. In addition, ablation only guided by EGM voltage may lead to unnecessary damage of functional myocardium not involved in VT.

Substrate mapping: Identification of slow conduction

Post-MI VTs are typically due to re-entry facilitated by slow conduction and fixed or functional conduction (pseudo-)block within the scar. (18) Accordingly, substrate-based ablation also relies on identification of EGMs consistent with slow conduction during SR that may be critical for VT circuits. Elimination of all EGMs with late or isolated components within the scar has been associated with improved ablation outcome. (15) However, in particular for fast VTs, slow conduction and block might be functional, only occurring at fast rates and short couplings intervals and hence, not detectable if mapping is performed during SR or continuous RV pacing only.(18,19) In a prior series, up to 33% of 100 post-MI patients referred for ablation did not have LPs. Of note, patients without LPs had typically smaller and less-dense scars. (15) Ablation of all EGMs poorly coupled to the rest of the myocardium (local abnormal ventricular activities [LAVAs]) has also been proposed. (14) The definition of LAVA includes, however, a broad spectrum of signals with low and high voltage sharp components occurring at any time before, during or after the far-field EGM. These EGMs might therefore be recorded in large areas. In addition, although in the work by Jais et al. the application of extrastimuli was used in some cases to detect LAVAs, neither the electrophysiological characteristics of LAVAs (e.g systematic evaluation of the response to RVE) nor their potential involvement in VT circuits was s studied systematically.-Of importance, in a recent study validated by simultaneous intraoperative activation mapping, EGMs with decremental conduction properties were more specifically associated with the diastolic VT pathway than LPs. (20) In our study, we restricted ablation to those EGMS exhibiting functional conduction delay or block during RVE (EDPs) aiming to reduce RF applications and to minimize the risk of damaging viable myocardium, in particular at those sites exhibiting normal BV during SR. Of note, LPs which did not delay further or block in response to RVE, indicating a fixed late activated area within the scar were not targeted. This approach translated into a median RF time of only 15 minutes, which is significantly shorter than reported for other substrate-based ablation strategies (**Supplementary Table 4**). Of note, the RF time was not different among groups despite the significant difference in scar size, suggesting that the size of the area exhibiting EDPs might be independent of the total scar size. Using EGM response to RVE for guiding substrate modification does not only increase the likelihood to identify relevant VT related sites, but also helped to identify ablation targets beyond the low BV area in 62% of the patients without prolonging the procedural time. Of importance, the identification an ablation of the hidden substrate in these patients with small and non-trasmural scars resulted in a lower incidence of VT recurrence on follow-up. On the contrary, patients with larger dense scars and overt slow conducting areas identified during SR did not benefit from additional substrate identification by RVE. In a recent small and heterogeneous group of patients undergoing ablation for scar-related VT, the value of the application of a double ventricular

extrastimulus for identifying additional slow conducting areas has been reported. (21) However, in contrast to our study, only sites with abnormal EGMs and particular characteristics (> 3 deflections, duration <133ms) were analysed, leading to underdetection of sites with functional delay hidden by normal EGMs (**Figure 1D**). The impact of this strategy on VT recurrence during follow-up was not reported.

Limitations

The major limitation of the study is its observational nature. Outcome comparison was performed with a historical cohort and although known determinants of VT recurrence (LV function, scar area) were matched, other uncontrolled factors may have influenced outcome. All procedures were performed by an experienced operator in a high volume centre which limits the generalization of the ablation results. Multipolar mapping catheters with small and narrow-spaced electrodes which may have improved far-field from near-field discrimination during SR were not used. Ventricular extrastimuli were always applied from the RV apex. Pacing from multiple sites (including LV) might have allowed identification of additional areas with EDPs. However, we expect the influence of the pacing site, especially for small scars, to be limited due to rapid activation of normal myocardium from the pacing site to the scar border. In addition, pacing from multiple LV sites would require an additional LV access and would likely prolong the procedure.

CONCLUSIONS

In patients with small and non-transmural scars after MI, systematic use of RVE during substrate mapping allows identification of areas of scar with functional conduction delay or block as substrate for VT that are not detectable if mapping is performed during SR or continuous RV pacing only. Ablation of this hidden substrate unmasked by RVE is associated with improved long-term procedural outcome.

Central Illustration.
Example of a patient from the hidden substrate group

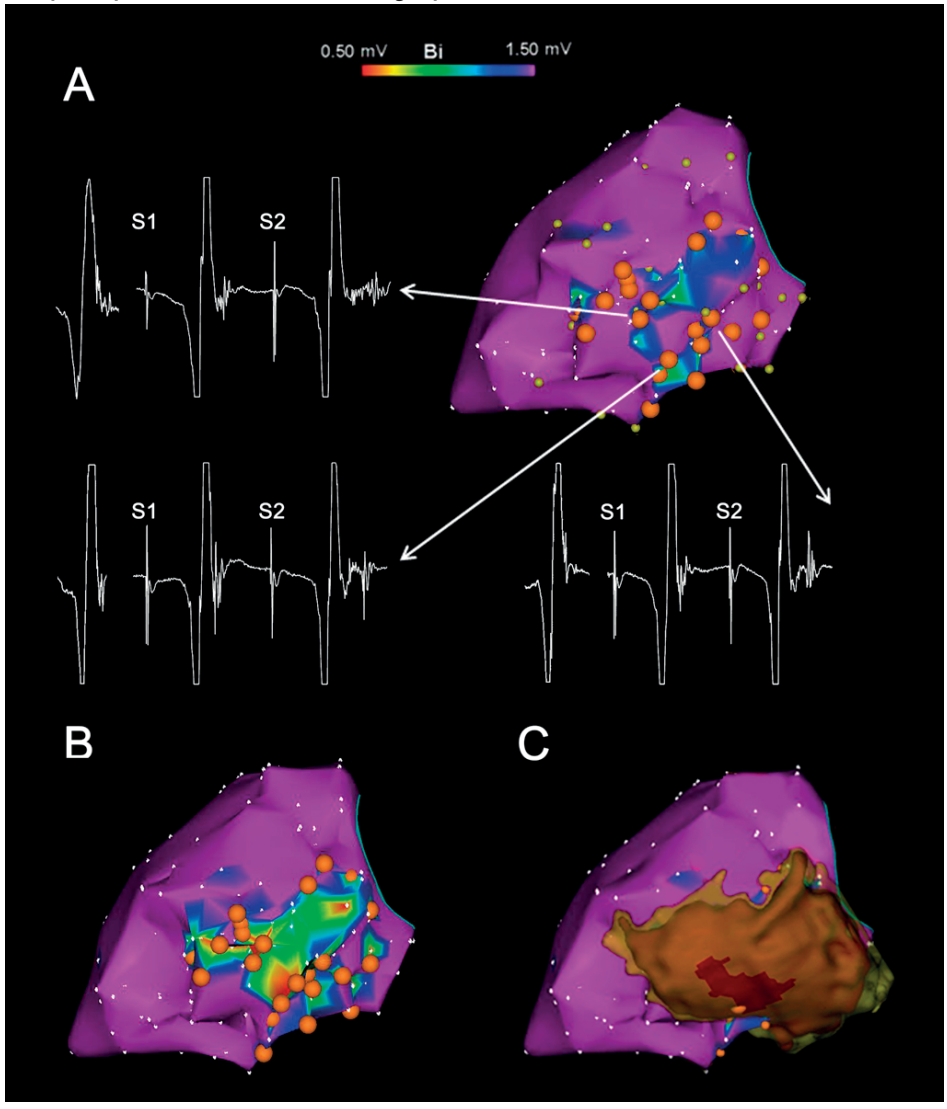

A: BV map (color-coded according to bar, left lateral view) showing a small lateral scar with no dense scar. Three EGMs recorded during SR and their response to RV pacing (S1) and RVE (S2) are shown. All three EGMs had normal amplitude. A high-frequency near-field potential is visible at the end of the far-field during SR. During RVE, conduction delay of the near-field is shown. These *Evoked Delayed Potentials* (EDPs) were targeted by ablation. Orange tags indicate EDPs. Other pacing sites are marked by yellow tags. **B:** Electroanatomical map corrected for the BV of the near-field EGM shows a better correlation with the CE-MRI segmented scar(C). **C:** 3D CE-MRI derived scar as registered with the voltage map. Scar border zone is displayed in yellow, scar core in brown and scar core with 100% transmurality in red. Note that EDPs outside the EA low BV area are located in areas of non-transmural scar.

REFERENCES

1. Marchlinski FE, Callans DJ, Gottlieb CD, Zado E. Linear ablation lesions for control of unmappable ventricular tachycardia in patients with ischemic and nonischemic cardiomyopathy. Circulation 2000;101:1288-96.
2. Zeppenfeld K, Kies P, Wijffels MC, Bootsma M, van Erven L, Schalij MJ. Identification of successful catheter ablation sites in patients with ventricular tachycardia based on electrogram characteristics during sinus rhythm. Heart rhythm 2005;2:940-50.
3. Berte B, Relan J, Sacher F et al. Impact of electrode type on mapping of scar-related VT. Journal of cardiovascular electrophysiology 2015.
4. Wijnmaalen AP, Schalij MJ, von der Thusen JH, Klautz RJ, Zeppenfeld K. Early reperfusion during acute myocardial infarction affects ventricular tachycardia characteristics and the chronic electroanatomic and histological substrate. Circulation 2010;121:1887-95.
5. Piers SR, Wijnmaalen AP, Borleffs CJ et al. Early reperfusion therapy affects inducibility, cycle length, and occurrence of ventricular tachycardia late after myocardial infarction. Circulation Arrhythmia and electrophysiology 2011;4:195-201.
6. Tung R, Josephson ME, Bradfield JS, Shivkumar K. Directional Influences of Ventricular Activation on Myocardial Scar Characterization: Voltage Mapping With Multiple Wavefronts During Ventricular Tachycardia Ablation. Circulation Arrhythmia and electrophysiology 2016;9.
7. Piers SR, Tao Q, de Riva Silva M et al. CMR-based identification of critical isthmus sites of ischemic and nonischemic ventricular tachycardia. JACC Cardiovascular imaging 2014;7:774-84.
8. van Huls van Taxis CF, Wijnmaalen AP, Piers SR, van der Geest RJ, Schalij MJ, Zeppenfeld K. Real-time integration of MDCT-derived coronary anatomy and epicardial fat: impact on epicardial electroanatomic mapping and ablation for ventricular arrhythmias. JACC Cardiovascular imaging 2013;6:42-52.
9. Watanabe M, de Riva M, Piers SRD et al. Fast nonclinical ventricular tachycardia inducible after ablation in patients with structural heart disease: Definition and clinical implications. Heart rhythm 2018.
10. de Riva M, Piers SR, Kapel GF et al. Reassessing noninducibility as ablation endpoint of post-infarction ventricular tachycardia: the impact of left ventricular function. Circulation Arrhythmia and electrophysiology 2015;8:853-62.
11. Arenal A, Hernandez J, Calvo D et al. Safety, long-term results, and predictors of recurrence after complete endocardial ventricular tachycardia substrate ablation in patients with previous myocardial infarction. The American journal of cardiology 2013;111:499-505.
12. Stevenson WG, Wilber DJ, Natale A et al. Irrigated radiofrequency catheter ablation guided by electroanatomic mapping for recurrent ventricular tachycardia after myocardial infarction: the multicenter thermocool ventricular tachycardia ablation trial. Circulation 2008;118:2773-82.
13. Di Biase L, Burkhardt JD, Lakkireddy D et al. Ablation of Stable VTs Versus Substrate Ablation in Ischemic Cardiomyopathy: The VISTA Randomized Multicenter Trial. Journal of the American College of Cardiology 2015;66:2872-2882.
14. Jais P, Maury P, Khairy P et al. Elimination of local abnormal ventricular activities: a new end point for substrate modification in patients with scar-related ventricular tachycardia. Circulation 2012;125:2184-96.
15. Tsiachris D, Silberbauer J, Maccabelli G et al. Electroanatomical voltage and morphology characteristics in postinfarction patients undergoing ventricular tachycardia ablation: pragmatic

approach favoring late potentials abolition. Circulation Arrhythmia and electrophysiology 2015;8:863-73.

16. Berte B, Sacher F, Cochet H et al. Postmyocarditis ventricular tachycardia in patients with epicardial-only scar: a specific entity requiring a specific approach. Journal of cardiovascular electrophysiology 2015;26:42-50.
17. Wijnmaalen AP, van der Geest RJ, van Huls van Taxis CF et al. Head-to-head comparison of contrast-enhanced magnetic resonance imaging and electroanatomical voltage mapping to assess post-infarct scar characteristics in patients with ventricular tachycardias: real-time image integration and reversed registration. European heart journal 2011;32:104-14.
18. Anter E, Tschabrunn CM, Buxton AE, Josephson ME. High-Resolution Mapping of Postinfarction Reentrant Ventricular Tachycardia: Electrophysiological Characterization of the Circuit. Circulation 2016;134:314-27.
19. Kawara T, Derksen R, de Groot JR et al. Activation delay after premature stimulation in chronically diseased human myocardium relates to the architecture of interstitial fibrosis. Circulation 2001;104:3069-75.
20. pacing site, especially for small scars, to be limited due to rapid activation of normal myocardium from the pacing site to the scar border. In addition, pacing from multiple LV sites would require an additional LV access and would likely prolong the procedure.

SUPPLEMENTARY METHODS

CE-MRI acquisition and processing

CE-MRI was performed on a 1.5-T Gyroscan ACS-NT/Intera or on a 3.0-T Ingenia MR system (Philips Medical Systems, Best, the Netherlands). A standardized clinical protocol was followed including cine MRI in long (2- and 4-chamber views) and short axis. Contrast enhanced images were acquired 15 min after bolus injection of gadolinium. The heart was either imaged in 1 or 2 breath-holds with 20 to 24 imaging levels in short and long axis views or with 20 to 26 imaging levels in the short axis view in one or two three-dimensional stacks, each stack acquired within one breathhold. Using in-house-developed MASS software (research version 3-1-2017; Medis; Leiden University Medical Center, Leiden, the Netherlands), the centreline of the left main, right coronary artery and the luminal boundary of the proximal aorta were manually defined. In the CE short-axis images, the endocardial and epicardial contours were semi-automatically detected. Scar was defined as myocardium with SI ≥35% of maximal myocardial SI, and was subdivided into core scar (≥50% of maximal SI) and border zone (35 to 50% of maximal SI). The LV anatomy, defined by the endocardial and epicardial contours was converted into 3D meshes using MASS software package. The scar anatomy was visualized as a 3D structure created with the MASS software. All meshes were imported into the Carto 3 system using CartoMerge image integration software (Biosense Webster Inc., Diamond Bar, California). After the procedure, all mapping points, including those categorized as EDPs, were projected onto the LGE MRI images using MASS software. For EDPs located within the CE-MRI derived scar, local transmurality of the scar was visually assessed.

Supplementary table 1: Baseline characteristics of the entire population

	All (n=150)	Historical group (n=90)	Study group (n=60)	*P-value*
Age, years	68 ± 9	68 ± 10	68 ± 8	0.907
Male	130 (87%)	81 (90%)	49 (82%)	0.151
Hypertension	60 (40%)	41 (46%)	19 (32%)	0.125
Diabetes Mellitus	23 (15%)	13 (14%)	10 (17%)	0.818
Prior stroke/TIA	13 (9%)	8 (9%)	5 (8%)	1.000
Atrial fibrillation	43 (29%)	28 (31%)	15 (25%)	0.465
Heart failure	63 (42%)	39 (43%)	24 (40%)	0.737
Renal failure	47 (31%)	29 (32%)	18 (30%)	0.858
Inferior MI	92 (61%)	57 (63%)	36 (60%)	0.864
Time since MI, year	19 ± 8	19 ± 9	19 ± 8	0.886
MI acute reperfusion	27 (18%)	15 (17%)	12 (20%)	0.667
Prior CABG	55 (37%)	37 (41%)	18 (30%)	0.226
Prior PCI	59 (39%)	35 (39%)	24 (40%)	1.000
LV ejection fraction, %	33 ± 12	34 ± 12	33 ± 12	0.632
ICD before ablation	106 (71%)	56 (62%)	50 (83%)	0.006
Prior VT ablation	24 (16%)	10 (11%)	14 (23%)	0.068
Clinical VT CL, ms	401 ± 93	391 ± 86	417 ± 102	0.101
Medication at admission				
Statins	133 (89%)	80 (89%)	53 (88%)	1.000
Antialdosteronic	48 (32%)	31 (34%)	17 (28%)	0.478
ACE-I/ARB	121 (81%)	75 (83%)	46 (77%)	0.399
Betablockers	116 (77%)	68 (76%)	48 (80%)	0.557
Amiodarone	60 (40%)	38 (42%)	22 (37%)	0.610
VT clinical presentation				
Electrical storm	22 (15%)	15 (17%)	7 (12%)	0.484
Incessant VT	19 (13%)	14 (16%)	5 (8%)	0.220
ICD therapies	38 (25%)	23 (26%)	15 (25%)	1.000
Below ICD detection	34 (23%)	10 (11%)	24 (40%)	<0.0001
First episode without ICD	37 (25%)	28 (31%)	9 (15%)	0.033

Values are reported as mean ± standard deviation or n (%). Abbreviations as in table 1.

Supplementary table 2: Procedural characteristics of the entire population

	All (n=150)	Historical group (n=90)	Study group (n=60)	*P-value*
Inducible before RFCA	139 (93%)	84 (93%)	55 (92%)	0.755
Number of induced VTs	3 (2–5)	3 (2–5)	3 (1–4)	0.129
Induced VT max CL, ms	420 ± 113	418 ± 117	420 ± 103	0.902
Induced VT min CL, ms	298 ± 78	295 ± 80	304 ± 78	0.511
LV bipolar scar area, cm^2	65 (41–87)	65 (41–88)	64 (41–87)	0.754
LV dense scar area, cm^2	24 (7–44)	23 (10–43)	25 (6–44)	0.661
LV border zone area, cm^2	35 (22–49)	36 (23–51)	34 (23–47)	0.743
Epicardial mapping	12 (8%)	6 (7%)	6 (10%)	0.544
Procedural duration, min	180 (150-225)	190 (145-235)	173 (150-205)	0.309
Fluoroscopic time, min	35 (24–48)	32 (23–48)	39 (33–47)	0.029
Radiofrequency time, min	15 (10-21)	15 (9-22)	15 (10-21)	0.997
Complications	19 (13%)	11 (12%)	8 (13%)	1.000
ICD after RFCA	129 (86%)	76 (84%)	53 (88%)	0.634
AADs at discharge				
Amiodarone	66 (44%)	43 (48%)	23 (38%)	0.314
Sotalol	41 (27%)	29 (32%)	12 (20%)	0.134
Class I	1 (1%)	0 (0%)	1 (2%)	0.400

Values are reported as mean ± standard deviation, median and IQR or n (%). Abbreviations as in table 3.

Supplementary table 3: Cox regression analysis for predictors of VT recurrence in the study group

	Hazard Ratio	95% CI	*P-value*
Absence of hidden substrate	4.63	1.41-15.15	0.011
Number of induced VTs (per VT)	1.24	1.01-1.52	0.039
LV ejection fraction per 1% increase	0.96	0.92-1.01	0.112
Bipolar scar area (per cm^2)	1.02	1.0-1.03	0.007
Non-inducibility after RFCA	0.87	0.28-2.65	0.799

CI indicates confidence interval. Rest of the abbreviations as in prior tables

Supplementary table 4:

First author and year of publication	Number of post-MI patients	Substrate ablation technique	Procedural time min	RF time min
Jaïs P. et al 2012(15)	56	LAVA elimination	148±73	23±11
Di Biase L. et al 2012(14)	92	Scar homogenization	288±90	74±21
Berruezo A. et al 2015(21)	75	Scar dechanneling	227±69	28±16
Tsiachris D. et al 2015(16)	100	Late potential abolition	243.1±72.4	28.9±14.7
Tzou W. et al 2015(22)	32	Core isolation	326±121	111±91
De Riva. et al 2017	60	EDP ablation	173 (150-205)	15 (10-21)

SUPPLEMENTARY REFERENCES

21. Berruezo, A., et al., *Scar dechanneling: new method for scar-related left ventricular tachycardia substrate ablation.* Circ Arrhythm Electrophysiol, 2015. **8**(2): p. 326-36.
22. Tzou, W.S., et al., *Core isolation of critical arrhythmia elements for treatment of multiple scar-based ventricular tachycardias.* Circ Arrhythm Electrophysiol, 2015. **8**(2): p. 353-61.